Quantum and temperature effects on Davydov soliton dynamics. II. The partial dressing state and comparisons between different methods

1993 J. Phys.: Condens. Matter 5 803

(http://iopscience.iop.org/0953-8984/5/7/008)

J. Phys.: Condens. Matter 5 (1993) 803–822. Printed in the UK

Quantum and temperature effects on Davydov soliton dynamics: II. The partial dressing state and comparisons between different methods

Wolfgang Förner

Department of Theoretical Chemistry, and Laboratory of the National Foundation of Cancer Research, Friedrich-Alexander University Erlangen-Nürnberg, Egerlandstrasse 3, W-8520 Erlangen, Federal Republic of Germany

Received 24 July 1992, in final form 30 October 1992

Abstract. In this work we report Davydov soliton dynamics at 300 K using the partial dressing *ansatz* state introduced by Brown and Ivic. As in the case of Davydov's $|D_1\rangle$ *ansatz* we found that the window for the appearance, in the partial dressing case, of slowly dispersing solitary waves in the parameter space is shifted to smaller non-linearities with increasing temperature. However, in the partial dressing approximation no stable solitons show up. Since the results of studies on the thermal stability of Davydov solitons using different models disagree with each other even qualitatively, we give some comparisons between results obtained using four different approximations to the dynamics with quantum Monte Carlo (QMC) results found in the literature. We find that Davydov's method ($|D_1\rangle$ state, averaged Hamiltonian) leads to quantitatively incorrect results, but reproduces the qualitative trends correctly. All other models considered by us ($|D_2\rangle$ state with thermal phonon population, Langevin equation and partial dressing state) failed to reproduce QMC results even qualitatively.

1. Introduction

Many biological processes are associated with an energy transfer through proteins, where this energy is released by hydrolysis of adenosine triphosphate (ATP). The mechanism of this energy transport is not quite clear. As an alternative to electronic mechanisms one can assume that the energy is stored as vibrational energy in the amide-I mode (CO stretch) of a polypeptide chain. Following Davydov's idea [1,2] one can take into account the coupling between the amide-I vibration and the acoustic phonons of the lattice. Through this coupling non-linear terms appear in the equations of motion. In this way the energy can be transported in solitary waves. Direct experimental evidence for the existence of such solitons in proteins is still missing. This is due to the complex structure of proteins, which makes such measurements very difficult. However, in acetanilide crystals a substructure with chains of hydrogen bonds similar to proteins is present. In low-temperature infrared and Raman spectra of this material a new band in the anide-I region appears. Up to now this band could only be explained with the help of a model similar to the Davydov soliton concept in proteins [3]. In this case the CO oscillators are coupled to optical phonons and the soliton would be pinned. Recent experiments, however, suggest that a conventional

0953-8984/93/070803+20$07.50

mode strongly coupled to the phonons might be responsible for the observed new band [4].

At zero temperature it has been confirmed theoretically that Davydov solitons exist for parameter values appropriate for proteins [5]. The investigation of temperature effects led to controversial results. Halding and Lomdahl [6] found stable pulses at $T = 310$ K using classical molecular dynamics for peptide units moving in a Lennard–Jones potential. Lomdahl and Kerr [7] and others [8] used the $|D_2\rangle$ *ansatz* together with a damping and a noise term to introduce temperature and found no stable solitons at 310 K at a specific set of parameters. Bolterauer [9] argued that their classical thermalization scheme might lead to too large a transfer of energy into the quantum system (oscillators). Cottingham and Schweitzer [10] applied perturbation theory to the Hamiltonian after partial diagonalization and could show (again for one set of parameters) that the soliton lifetime at 300 K is too short for biological processes. In our previous work [11–13] we prepared the lattice in a thermally excited state prior to the soliton starting. We compared our results with those of [7] and found agreement between the models if in the Langevin model [7] the lattice is thermally equilibrated before the soliton starts. We could show that in a window in the parameter space, which might well be realistic for proteins, travelling solitons exist at 300 K (see also [14] for a recent review).

Brown *et al* [15] have shown that the $|D_2\rangle$ state *ansatz* does not reproduce the dynamics of the exactly solvable small-polaron limit (dipole–dipole coupling neglected). Davydov [2] introduced a more sophisticated *ansatz* state ($|D_1\rangle$), which allows for quantum effects in the lattice. However, he used the energy expectation value for $|D_1\rangle$ as classical Hamiltonian function to derive equations of motion [2]. It was shown that with these equations $|D_1\rangle$ does not reproduce the small-polaron limit [15] either. With these equations of motion and a thermally averaged Hamiltonian, Davydov [2] could show within the continuum limit that solitons exist at 300 K. Cruzeiro *et al* [16] reached the same conclusion numerically without making use of Davydov's approximations, but using also the thermally averaged Hamiltonian as a classical Hamiltonian function. Brown and Ivic [17] have introduced a third *ansatz* state in which the phase mixing ('dressing') between the amide-I oscillators and the lattice phonons is intermediate between the classical $|D_2\rangle$ and the quantum $|D_1\rangle$ *ansatz* of Davydov. We found [18] that using this state at $T = 0$ K no travelling solitons exist, but only dispersing waves were found for a non-linearity parameter less than 300 pN (for proteins this parameter is usually assumed to be around 60 pN). In this work we present numerical results obtained using the partial dressing *ansatz* at 300 K. This *ansatz* is interesting since at 0 K the results are qualitatively similar (appearance of coherent structures at very high non-linearities in both models) to those from the better $|D_1\rangle$ state and, in contrast to $|D_1\rangle$, from the partial dressing state analytical results can be derived in the continuum limit [17]. Further, the inclusion of temperature effects into the partial dressing model is more straightforward than in the $|D_1\rangle$ case.

Mechtly and Shaw [19] and Skrinjar *et al* [20] could derive new equations of motion for $|D_1\rangle$ with the help of quantum-mechanical methods. These equations of motion reproduce the small-polaron limit. However, in the general case, also this *ansatz* state is still approximative. In [19] as well as in our work [18] it is shown that at $T = 0$ K the window for travelling solitons in the $|D_1\rangle$ state occurs in regions of the parameter space that cannot be applied to proteins (soliton formation threshold $X > 150$ pN). In the first paper of this series [21] we also used the Langrangian

method described in [20] to obtain correct equations of motion for the $|D_1\rangle$ *ansatz* state from the thermally averaged Hamiltonian derived in [2, 16]. In this investigation [21, 22], as well as in our previous studies using the $|D_2\rangle$ state, summarized in [22], we found that Davydov solitons should be stable at 300 K if the spring constant of the hydrogen bonds is larger than previously assumed. There are doubts if the Davydov concept of using a thermally averaged Hamiltonian to derive equations of motion from it is in agreement with statistical mechanics. There is the possibility that it may lead to results that are even qualitatively misleading. Therefore we present in section 4 a comparison of our results obtained with different models with the exact quantum Monte Carlo results of Wang *et al* [23].

2. Methods

2.1. The Hamiltonian

The Hamiltonian as introduced by Davydov [1] is

$$\hat{H} = \sum_n \left(E_0 \hat{a}_n^+ \hat{a}_n - J_n(\hat{a}_n^+ \hat{a}_{n+1} + \hat{a}_{n+1}^+ \hat{a}_n) + \frac{\hat{p}_n^2}{2M_n} + \frac{W_n}{2}(\hat{q}_{n+1} - \hat{q}_n)^2 + X_n \hat{a}_n^+ \hat{a}_n (\hat{q}_{n+1} - \hat{q}_n) \right). \tag{1}$$

In equation (1) $\hat{a}_n^+$ ($\hat{a}_n$) are the usual boson creation (annihilation) operators [5] for the amide-I oscillators at sites n (see figure 1). From infrared spectra the excitation energy of an isolated amide-I oscillator can be deduced ($E_0 = 0.205$ eV). Usually for all parameters in equation (1) site-independent mean values are used. The average value for the dipole–dipole coupling between neighbouring amide-I oscillators is $J = 0.967$ meV. The average spring constant of the hydrogen bonds is usually taken to be $W = 13$ N m^{-1} from crystalline formamide where the molecules also form hydrogen-bonded chains. In our preliminary paper [11] we used $W = 76$ N m^{-1}, which is the spring constant for the hydrogen bonds in the hydrogen carbonate dimer, $\hat{p}_n$ is the momentum and $\hat{q}_n$ the position operator of unit n. The average mass M is taken as that of myosine ($M = 114 m_p$, m_p = proton mass). The energy of the CO stretching vibration with the oxygen atom taking part in hydrogen bonds is a function of the length r of the hydrogen bond ($E = E_0 + Xr$). For X the experimental estimates are 35 and 62 pN. *Ab initio* calculations on formamide dimers usually lead to $X = 30$–50 pN (see e.g. [14] for a review and references). In the case of comparisons with quantum Monte Carlo results [23] we had to introduce in addition to cyclic boundary conditions also the so-called symmetric interaction. In this case the oscillator–lattice interaction term is given by (assuming X to be equal for both hydrogen bonds neighbouring an amide-I oscillator)

$$\hat{V}_{\text{Int}} = X \sum_n \hat{a}_n^+ \hat{a}_n (\hat{q}_{n+1} - \hat{q}_{n-1}) \tag{2}$$

which is usually considered as rather unrealistic; however, it was used in [23] and thus we had to introduce it also in order to make comparison possible.

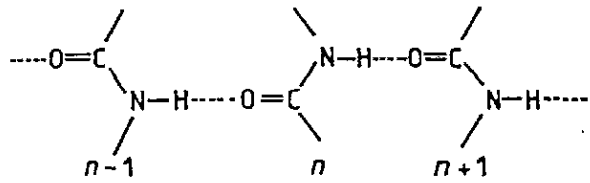

Figure 1. Schematic picture of a hydrogen-bonded channel in a protein.

The Hamiltonian [1, 2] in second quantized form including disorder is given by

$$\hat{H} = \sum_n [E_0 \hat{a}_n^+ \hat{a}_n - J_n(\hat{a}_{n+1}^+ \hat{a}_n + \hat{a}_n^+ \hat{a}_{n+1})]$$
$$+ \sum_k \hbar\omega_k \left(\hat{b}_k^+ \hat{b}_k + \tfrac{1}{2} + \sum_n B_{nk}(\hat{b}_k + \hat{b}_k^+)\hat{a}_n^+ \hat{a}_n \right) \tag{3}$$

$$B_{nk} = \frac{X_n}{\omega_k} \left(\frac{1}{2\hbar\omega_k} \right)^{1/2} \left(\frac{U_{n+1,k}}{M_{n+1}^{1/2}} - \frac{U_{nk}}{M_n^{1/2}} \right).$$

$\hat{b}_k^+$ ($\hat{b}_k$) are creation (annihilation) operators for acoustic phonons of wavenumber k. The translational mode has to be excluded from the summation. Note that in equation (3) we use again the asymmetric interaction model where only the coupling of the oscillator n to the hydrogen bond between n and $n+1$ in which the oscillator takes part is considered. Here ω_k denotes the eigenfrequency of the normal mode k and **U** contains the normal mode coefficients. ω and **U** are obtained by numerical diagonalization of the matrix **V** with elements

$$V_{nm} = \{[W_n(1-\delta_{nN}) + W_{n-1}(1-\delta_{n1})]\delta_{nm}$$
$$- W_n(1-\delta_{nN})\delta_{m,n+1} - W_{n-1}(1-\delta_{n1})\delta_{m,n-1}\}(M_n M_m)^{-1/2}. \tag{4}$$

The form of **V** implies that we use free chain ends and N units. Cyclic boundary conditions [16], which we need for comparisons with [23], lead to the form

$$V_{nm} = \{[W_n + W_{n-1}]\delta_{nm} - W_n\delta_{m,n+1} - W_{n-1}\delta_{m,n-1}\}(M_n M_m)^{-1/2} \tag{5}$$

for this matrix, where now the site indices have to be taken modulo N. For the symmetric interaction the matrix **B** is given by

$$B_{nk} = \frac{X}{\omega_k} \left(\frac{1}{2\hbar\omega_k} \right)^{1/2} \left(\frac{U_{n+1,k}}{M_{n+1}^{1/2}} - \frac{U_{n-1,k}}{M_{n-1}^{1/2}} \right). \tag{6}$$

For the solution of the time-dependent Schrödinger equation in the literature different *ansatz* states can be found, as well as different models for the inclusion of temperature effects. Those which we applied in this work will be briefly described in the following subsections.

2.2. The $|D_2\rangle$ ansatz state

The most simple possible *ansatz* is the displaced oscillator state *ansatz* ($|D_2\rangle$) of Davydov [1]:

$$|D_2\rangle = \sum_n a_n'(t)\hat{a}_n^+|0\rangle_e \exp\left(\sum_k [b_k(t)\hat{b}_k^+ - b_k^*(t)\hat{b}_k]\right)|0\rangle_p. \tag{7}$$

Here $a_n'(t)$ is the probability to find a vibrational quantum at site n, and the b_k are the coherent state amplitudes for normal mode k. Thus in this *ansatz* it is assumed that the oscillators, regardless of their excitation state, create via the interaction the same number of vibrational quanta in the normal modes of the lattice. In this approximation the lattice variables are treated classically. In (7), $|0\rangle_e$ denotes the exciton vacuum and $|0\rangle_p$ the phonon vacuum. Davydov [1, 2] formed the expectation value of the Hamiltonian (1) with $|D_2\rangle$ and used this expectation value as classical Hamiltonian function. In this way he obtained the equations of motion. Kerr and Lomdahl [24] have shown that these equations can be obtained also by purely quantum-mechanical methods and also for states of more than one quantum [25]. Explicit forms of the equations of motion without inclusion of temperature effects can be found in [12, 13]. The $|D_2\rangle$ state reproduces the lattice dynamics for $J = 0$ correctly, but leads to an incorrect phonon energy [15]. In the next two subsections two models for the inclusion of temperature into this *ansatz* state, which are used in this work, are described.

2.2.1. Thermal population of the lattice phonons. In our model for the inclusion of temperature effects we first solve the decoupled lattice problem ($X = 0$) [13], which is simply a chain of coupled harmonic oscillators. As initial excitations we distribute an energy of Nk_BT (k_B is Boltzmann's constant) on the normal modes using Bose–Einstein statistics. Half of this energy was distributed as potential, the other half as kinetic energy. The analytically given lattice displacements due to thermal motion are separated from the ones originating from exciton–phonon coupling (see [12, 13, 22] for details of the formalism).

In this way the heat bath introduces two oscillating phase factors at J. These oscillations occur in both space and time. The spatial oscillation is due to the normal mode coefficients. With increasing temperature the admixture of higher normal modes increases, which have more spatial oscillations due to their larger number of nodes. Thus temperature has the same net effect as disorder in the site energy E_0, which can be played back to exactly the same mathematical structure [12]. However, in addition we have here also oscillations in time, which become faster with increasing temperature due to the higher frequencies (ω_k), which become more important. Since the phases at J are proportional to the coupling constant X one expects a threshold value for X. If X becomes larger than this threshold the soliton should be destroyed.

2.2.2. Langevin equation. In the Langevin *ansatz* for the treatment of temperature as reported by Lomdahl and Kerr [7, 24, 25], a damping and a random force term are added to the equations of motion:

$$\begin{aligned} i\hbar\dot{a}_n &= -J(a_{n+1} + a_{n-1}) + X(q_{n+1} - q_{n-1})a_n \\ M\ddot{q}_n &= W(q_{n+1} - 2q_n + q_{n-1}) + X(|a_{n+1}|^2 - |a_{n-1}|^2) - M\Gamma\dot{q}_n + F_n(t). \end{aligned} \tag{8}$$

Note that here we have already introduced the symmetric interaction term necessary for the comparison with QMC results [23]. The correlation function for the random forces is

$$\langle F(x,t)F(0,0)\rangle = 2Mk_{\mathrm{B}}T\Gamma[\delta(x)/a]\delta(t) \tag{9}$$

(a is the lattice constant). In this case our equation of motion for the lattice displacements becomes a Langevin equation. The random forces are assumed to follow a normal normal distribution. The effect of the two additional terms in the equations of motion is to drive the system into thermal equilibrium with a time constant Γ. For the time constant we use the lowest non-zero phonon frequency of the lattice as suggested by Lomdahl and Kerr [7, 24, 25]

$$\Gamma = \nu_{\min} = \frac{\omega_{\min}}{2\pi}. \tag{10}$$

2.3. The $|D_1\rangle$ *ansatz state*

The $|D_1\rangle$ *ansatz* for inclusion of temperature in Davydov's approximation for solution of the time-dependent Schrödinger equation is

$$|D_1,\nu\rangle = \sum_n a'_n(t)\hat{a}_n^+|0\rangle_e|\beta_n,\nu\rangle. \tag{11}$$

Here again $|0\rangle_e$ is the exciton vacuum, and $|\beta_n,\nu\rangle$ a coherent phonon state. For the one-quantum oscillator states used here $\sum_n |a'_n|^2 = 1$ holds. To include temperature approximately we assume, as in [16] that a phonon distribution is present in the lattice where each normal mode is occupied by ν_k quanta. All possible distributions $|\nu\rangle$ are considered in the thermal average of the Hamiltonian. We do not consider a thermal distribution of amide-I quanta since at 300 K the Boltzmann factor implies that only 3 of 10 000 amide-I oscillations would be thermally excited. Thus one can neglect a possible thermalized soliton distribution in the system too, since presence of solitons requires first of all amide-I excitation. Then

$$|\beta_n,\nu\rangle = \exp\left(\sum_k [b_{nk}(t)\hat{b}_k^+ - b_{nk}^*(t)\hat{b}_k]\right)|\nu\rangle \tag{12}$$

where the $b_{nk}(t)$ are the coherent state amplitudes. The equations of motion are derived with the Euler–Lagrange formalism following [20] and are given in detail in [18, 21]. This method introduced by Davydov was criticized by several authors as being inconsistent with statistical mechanics, since equations of motion are obtained from a thermally averaged Hamiltonian. However, we feel that it might still be a reliable approximation to the real dynamics under physiological temperature. To investigate this we also performed with this method a comparison with quantum Monte Carlo simulations.

2.4. The partial dressing ansatz

Brown and Ivic [17] have introduced a modified *ansatz* state, which is called the $|D\rangle$ or partial dressing state. The $|D\rangle$ states are a subset of the $|D_1\rangle$ states discussed above, where a fixed degree of phase mixing between phonons and excitons is incorporated [17]:

$$|D\rangle = \sum_n a'_n(t)\hat{a}_n^{+\prime}|0\rangle_e \exp\left(\sum_k [b'_k(t)\hat{b}_k^{+\prime} - b_k^{*\prime}(t)\hat{b}'_k]\right)|0\rangle_p. \tag{13}$$

Here the operators are given by

$$\begin{aligned} \hat{a}'_n &= \hat{a}_n \exp\left(\delta \sum_k B_{nk}(\hat{b}_k^{+\prime} - \hat{b}'_k)\right) \\ \hat{b}'_k &= \hat{b}_k + \delta \sum_n B_{nk}\hat{a}_n^+ \hat{a}_n \end{aligned} \tag{14}$$

and δ is the dressing factor. The coefficients in the $|D\rangle$ state are related to those in $|D_1\rangle$ by

$$\begin{aligned} a_n(t) &= a'_n(t) \exp\left(-\tfrac{1}{2}\delta \sum_k B_{nk}[b'_k(t) - b_k^{*\prime}(t)]\right) \\ b_{nk}(t) &= -\delta B_{nk} + b'_k(t). \end{aligned} \tag{15}$$

In this expression we used the fact that **B** is real or can be chosen as real via the phases of the normal modes. The total energy is given by

$$\begin{aligned} E_t = \sum_n [E_0 - \delta(2-\delta)f_n]|a'_n|^2 &+ \sum_k \hbar\omega_k \left(|b'_k|^2 + \tfrac{1}{2}\right) \\ &- \sum_n a_n^{*\prime}(J'_n a'_{n+1} + J'_{n-1}a'_{n-1}) \\ &+ 2(1-\delta)\sum_k \hbar\omega_k B_{nk}\mathrm{Re}(b'_k)|a'_n|^2 \end{aligned} \tag{16}$$

the small-polaron binding energy f_n by [17]

$$f_n = \sum_k B_{nk}^2 \hbar\omega_k \tag{17}$$

and the scaled oscilator coupling by

$$J'_n = J_n \exp\left(-\tfrac{1}{2}\delta^2 \sum_k (B_{nk} - B_{n+1,k})^2\right). \tag{18}$$

The dressing factor δ can be obtained by minimization of the averaged total energy [17] according to equation (4.12) of [17]. We have computed δ for $T = 0$ K in a periodic chain. The results [18] show that for 0.8 meV $< J <$ 1.2 meV δ varies

between 0.76 and 0.97, where δ decreases with increasing J. With increasing nonlinearity δ increases also; however, the larger W becomes, the smaller is the variation in δ, and the larger is its value. Thus for increasing J and decreasing X and W the $|D\rangle$ state approaches the $|D_2\rangle$ state ($\delta = 0$), while for decreasing J and increasing X and W the $|D\rangle$ state approaches the small-polaron limit ($\delta = 1$). For $J = 0.967$ meV and $W = 10$ N m^{-1}, δ varies by $\simeq 0.15$ in the range $0 < X < 200$ pN. For $X = 0$, $\delta \simeq 0.796$ is obtained; and for $X = 200$ pN, $\delta \simeq 0.944$. For $X = 60$ pN we obtain in agreement with Brown and Ivic [17] $\delta \simeq 0.81$. Thus for the usually used values of the parameters the $|D\rangle$ state is closer to the small-polaron limit than to the $|D_2\rangle$ state.

Brown and Ivic [17] derived the equations of motion for the $|D\rangle$ state with the help of the time-dependent variational principle. However, in their equations for the time derivative of a'_n this variable occurs also on the right-hand side as an integrand. Thus numerical simulations would be difficult. The term that leads to technical difficulties appears in the equation for $b'_k(t)$ in [17]:

$$\int_0^t \exp[-i\omega_k(t-t')] \sum_n B_{nk} \frac{d}{dt'} |a'_n(t')|^2 \, dt'. \tag{19}$$

Integration by parts yields

$$\begin{aligned} &- i\omega_k \int_0^t \exp[-i\omega_k(t-t')] \sum_n B_{nk} |a'_n(t)|^2 \, dt' + \sum_k B_{nk} |a'_n(t)|^2 \\ &- \exp(-i\omega_k t) \sum_n B_{nk} |a'_n(0)|^2. \end{aligned} \tag{20}$$

Thus $b'_k(t)$ is finally given by

$$\begin{aligned} b'_k(t) = &\left(b'_k(0) - \delta \sum_n B_{nk} |a'_n(0)|^2 \right) \exp(-i\omega_k t) + \delta \sum_n B_{nk} |a'_n(t)|^2 \\ &- i\omega_k \int_0^t \exp[i\omega_k(t-t')] \sum_n B_{nk} |a'_n(t')|^2 \, dt'. \end{aligned} \tag{21}$$

For numerical simulations a suitably small time step τ is introduced. During this time step (or half of it as in the Runge–Kutta method) the integrand is linearly interpolated. Thus at time $l\tau$ we obtain

$$b'_k(l) = A_k \exp(-i\omega_k l\tau) + C_k(l) - i\omega_k \exp(-i\omega_k l\tau) \sum_n B_{nk} D_{nk}(l) \tag{22}$$

where

$$\begin{aligned} A_k &= b'_k(0) - \delta \sum_n B_{nk} |a'_n(0)|^2 \\ C_k(l) &= \delta \sum_n B_{nk} |a'_n(l)|^2 \end{aligned} \tag{23}$$

and

$$\begin{aligned} D_{nk}(l) &= D_{nk}(l-1) + (\tau/2)[E_{nk}(l) + E_{nk}(l-1)] \\ D_{nk}(0) &= 0 \\ E_{nk}(l) &= \exp(\mathrm{i}\omega_k l\tau)|a'_n(l)|^2. \end{aligned} \tag{24}$$

For $T = 0$ K the initial phonon data are $b'_k(0) = 0$. After computation of $a'_n(l)$ and $b'_k(l)$ at time $l\tau$ the time derivative of $a'_n(l)$ can be calculated,

$$\begin{aligned} \mathrm{i}\hbar\dot{a}'_n(l) = {} & [E_0 - \delta(2-\delta)f_n]a'_n(l) - J'_n a'_{n+1}(l) - J'_{n-1}a'_{n-1}(l) \\ & + 2\sum_k \hbar\omega_k B_{nk}\mathrm{Re}[b'_k(l)]a'_n(l) \\ & + 2\delta(1-\delta)\sum_{mk}\hbar\omega_k B_{nk}B_{mk}|a'_m(l)|^2 a'_n(l). \end{aligned} \tag{25}$$

Note that $\mathrm{Re}[x]$ and $\mathrm{Im}[x]$ denote real and imaginary part, respectively, of quantity x. From the time derivative of $a'_n(l)$ then $a'_n(l+1)$ can be computed and then $b'_k(l+1)$. In practice, as usual a gauge transformation is performed,

$$a''_n(t) = a'_n(t)\exp[\mathrm{i}(E_0/\hbar)t] \tag{26}$$

which removes the term containing E_0 and thus the fast oscillating part of a'_n. Finally from $b_{nk} = -\delta B_{nk} + b'_k$ the momenta p_n and displacements q_n of the lattice units can be obtained:

$$\begin{aligned} p_n(l) &= \sum_{mk}(2\hbar M_n\omega_k)^{1/2}U_{nk}|a_m(l)|^2\,\mathrm{Im}[b_{mk}(l)] \\ q_n(l) &= \sum_{mk}\left(\frac{2\hbar}{M_n\omega_k}\right)^{1/2}U_{nk}|a_m(l)|^2\,\mathrm{Re}[b_{mk}(l)]. \end{aligned} \tag{27}$$

Typically a time step of $\tau = 5$ fs was used in our simulations at $T = 0$ K [18] with a Runge–Kutta method correct up to fourth order. In typical cases ($M = 114m_p$, $W = 13$ N m^{-1}, $J = 0.967$ meV, $X = 240$ pN) for a periodic chain of 50 units within 70 ps the error in total energy was less than 50 μeV ($\simeq 0.02\%\ E_t$) and the norm is conserved to better than 4×10^{-4}. In this case $\delta = 0.9016$ and the translational mode was kept unpopulated.

As already discussed in the paper by Brown and Ivic [17] the inclusion of temperature enters in the determination of δ, where a thermal average is involved, via the quantity

$$S_n(t) = \tfrac{1}{2}\sum_k (B_{nk} - B_{n-1,k})^2 \coth\left(\frac{\hbar\omega_k}{2k_B T}\right) \tag{28}$$

and thus in J_n in form of a Debye–Waller factor

$$J'_n(T) = J_n \exp[-\delta^2 S_n(t)]. \tag{29}$$

Further in the equations of motion temperature appears directly in the phonon initial data $b'_k(0)$. Approximately these can be obtained in the same way as for $|D_2\rangle$ dynamics. One can populate all modes (except the translational one) of the lattice corresponding to a Bose–Einstein distribution and solve the dynamical problem of the decoupled lattice. With p_n and q_n at some arbitrary time t_0 (the results do not depend on t_0 as shown previously [11]) one can calculate (for uniform masses: $M_n = M$)

$$\begin{aligned} \mathrm{Re}[b'_k(0)] &= \sum_n \left(\frac{M\omega_k}{2\hbar}\right)^{1/2} U_{nk} q_n(t_0) \\ \mathrm{Im}[b'_k(0)] &= \sum_n \left(\frac{1}{2\hbar M\omega_k}\right)^{1/2} U_{nk} p_n(t_0) \end{aligned} \tag{30}$$

and use these values as input for the time simulation. As in the case of $|D_1\rangle$ dynamics one has to note that, the larger X is, the smaller the time step has to be chosen.

In previous work we have shown [18] that in contrast to $|D_2\rangle$ and $|D_1\rangle$ no real travelling soliton shows up. Only from $X = 180$ pN can one speak of a slowly dispersive solitary wave. For $X = 260$ pN a pinned soliton is observed numerically at $T = 0$ K. For the $|D\rangle$ state the parameter space that allows soliton formation is very small and at rather large values of X. Thus if the $|D\rangle$ state were to be a better approximation to the exact solution than $|D_2\rangle$ or $|D_1\rangle$ one would have to conclude that the Davydov soliton cannot exist in proteins already at $T = 0$ K. However, the $|D\rangle$ states are a subset of the $|D_1\rangle$ states and the $|D_1\rangle$ equations [18, 20] are derived with the time-dependent variational principle as well as the $|D\rangle$ states [17]. Therefore the $|D_1\rangle$ dynamics should be a better approximation to the exact ones than the $|D\rangle$ dynamics. If the $|D\rangle$ dynamics were to approximate the exact solution better, then $|D_1\rangle$ dynamics would numerically reduce to $|D\rangle$ dynamics, which is not the case. But since the general trend concerning soliton stability regions is qualitatively similar in $|D\rangle$ and $|D_1\rangle$ dynamics, the partial dressing state is still an important approximation since in contrast to $|D_1\rangle$ it allows analytical considerations in the continuum limit [17]. Therefore it is worth while to study temperature effects also in the $|D\rangle$ approximation, which is the subject of the next section. We could reproduce the δ value for $T = 0$ K given in [17] (cyclic chain, symmetric interaction, numerical calculation of eigenvectors and eigenfrequencies) for a chain of 1000 (δ depends on the chain length) sites to an accuracy of three digits and for $T = 300$ K we find $\delta = 0.43$.

3. Effects of temperature in the partial dressing state

We have performed dynamic simulations on chains of 50 units starting from a one-site excitation at unit 49 at a temperature of 300 K using the asymmetric interaction *ansatz* and free chain ends. The time step was 5 fs and the norm was conserved during a typical simulation through 24 ps ($M = 114m_p$, $J = 0.967$ meV, $X = 140$ pN, $W = 30$ N m^{-1}, $T = 300$ K) to better than 4×10^{-4}; the energy error was less than 70 μeV. In this case the dressing factor was 0.648 and the simulation time for one run on our Cyber 995E computer was 600 CPU seconds. These errors become somewhat larger for larger X and very much smaller for smaller X (e.g. in case of

$X = 60$ pN the dressing factor is 0.588, the norm error less than 3×10^{-6}, and the energy error less than 0.3 μeV). We varied the values of W and X. The results are shown in figure 2, where each circle corresponds to a simulation performed.

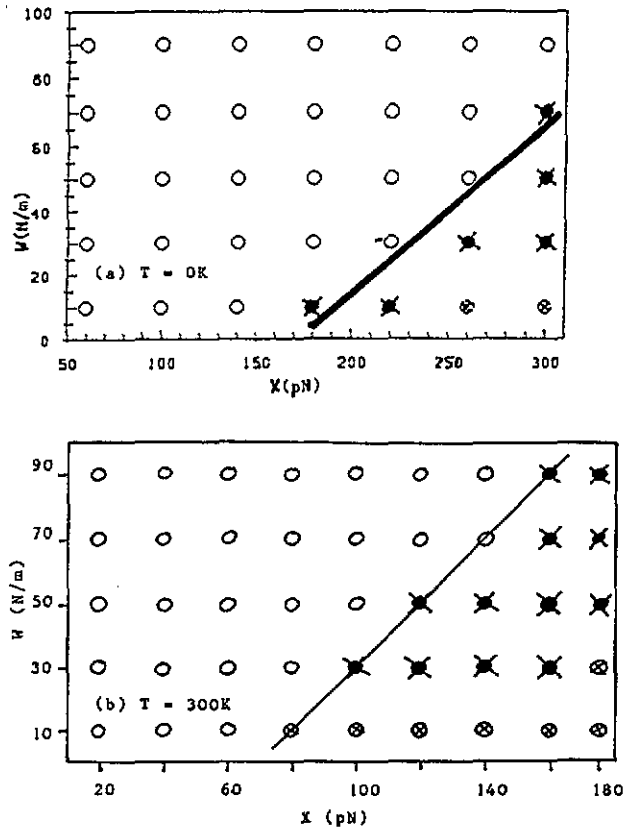

Figure 2. Survey of the (X, W) parameter space using the partial dressing model at (*a*) $T = 0$ K (*b*) $T = 300$ K (open circles denote dispersive behaviour of the initial excitation, crossed black circles indicate formation of slowly dispering solitary waves and crossed open circles indicate pinning of the initial excitation). All simulations started from a one-site excitation and the asymmetric interaction as well as free chain ends were used.

We show the results for 300 K together with those for 0 K published previously [18]. It is obvious from the figure that for both temperatures no true solitons could be observed. However, in the $|D\rangle$ state model the same phenomenon as for the $|D_1\rangle$ *ansatz* is present: the soliton or in this case solitary wave stability window is shifted to smaller values of X when the temperature increases. Also at high temperature the region of pinned excitations is much larger than at 0 K. The border between regions of dispersing and localized excitations is for both temperatures roughly linear. This border line becomes shifted by roughly -80 pN in X in a nearly parallel way when temperature increases. Thus the basic discrepancies between $|D\rangle$ and $|D_1\rangle$ are, first, that in the $|D\rangle$ model only solitary waves show up while in the $|D_1\rangle$ state also stable solitons are present, and, secondly, that the shift of solitary wave stability to smaller

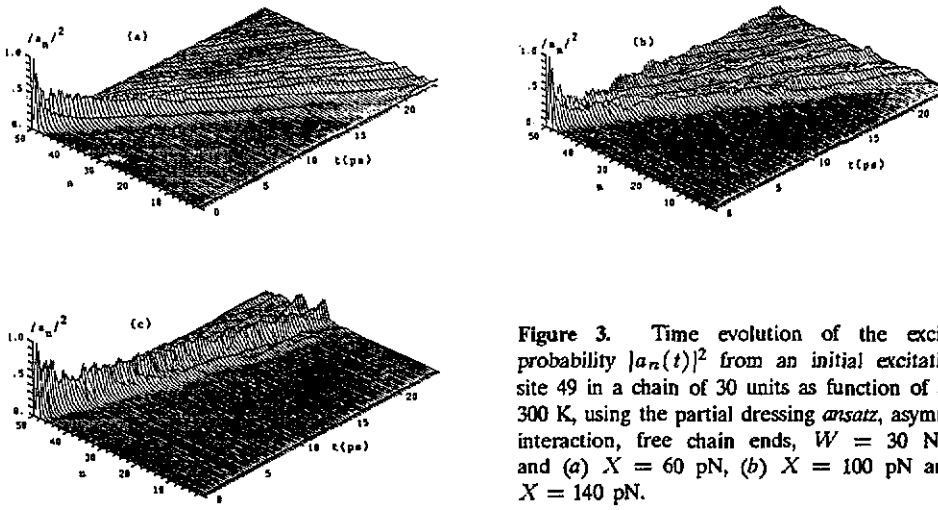

Figure 3. Time evolution of the excitation probability $|a_n(t)|^2$ from an initial excitation at site 49 in a chain of 30 units as function of site at 300 K, using the partial dressing *ansatz*, asymmetric interaction, free chain ends, $W = 30$ N m^{-1} and (*a*) $X = 60$ pN, (*b*) $X = 100$ pN and (*c*) $X = 140$ pN.

X values with increasing temperature is less pronounced in the $|D\rangle$ state compared to $|D_1\rangle$.

In figure 3 we show some explicit examples of the dynamics obtained for $W = 30$ N m^{-1} and some values of X. Figure 3(*a*) shows an example of clearly dispersive behaviour for $X = 60$ pN. For $X = 100$ pN (figure 3(*b*)) we see that a dispersive solitary wave is formed, which has already lost most of its intensity after 24 ps. At $X = 140$ pN (figure 3(*c*)) the solitary wave is more stable and its velocity much reduced. However, it is obvious that it is still slowly dispersing. Close to the end of the simulation it seems that it splits into two separate waves where one is moving further into the chain while the second one seems to be pinned.

Obviously there is some very qualitative similarity between the results obtained with the $|D\rangle$ and the $|D_1\rangle$ state. The advantages of the $|D\rangle$ state *ansatz* are clearly that the introduction of temperature effects is straightforward and that in the continuum limit analytical solutions can be obtained. Both are not the case for the $|D_1\rangle$ state *ansatz*. However, it seems from the results that the higher flexibility of the $|D_1\rangle$ state concerning the coherent state amplitudes leads to conclusions that differ considerably from those drawn from the $|D\rangle$ state simulations. Therefore it might be dangerous to use, for example, analytical $|D\rangle$ state results to discuss properties of Davydov solitons or the question of their thermal stability. However, the temperature model introduced by Davydov for $|D_1\rangle$ is considered to be inconsistent with statistical mechanics. Since it might still give qualitatively correct results we present in the next section a comparison of different dynamic models for the inclusion of temperature effects with known exact results from quantum Monte Carlo calculations reported by Wang *et al* [23].

4. Comparisons with exact quantum Monte Carlo results

Wang *et al* [23] reported the results of quantum Monte Carlo (QMC) simulations on the Davydov Hamiltonian. These results should describe the equilibrium state in principle exactly, restricted only by numerical inaccuracies, which can be controlled. They applied the parameters usually used in the literature ($J = 0.967$ meV,

$W = 13$ N m^{-1}, $X = 62$ pN, $M = 114m_p$), cyclic boundaries, the symmetric interaction, and rings of 25 sites. They determined for each of their configurations the excitation site n_0, and rotated all coordinates such that this site is in the middle of their lattice. Then they computed the average $\langle A_n \rangle$ of the lattice displacements

$$A_n = q_{n+1} - q_{n-1}. \tag{31}$$

Here n refers to the rotated coordinate system, where the excitation site n_0 is always in the centre. We implemented cyclic boundaries and symmetric interaction into our time simulation programs, started from a random distribution of one amide-I vibrational quantum and performed a time average of the same quantity with which Wang *et al* performed their ensemble average. We determined n_0 in each time step as the site where the excitation probability $|a_n(t)|^2$ is largest. In this way after a sufficient number of time steps (convergence of $\langle A_n \rangle$) we should obtain results comparable with those of Wang *et al* [23]. We want to emphasize again that, in order to make this comparison possible, we used for all computations reported below the symmetric interaction and cyclic boundary conditions. In [23] it is reported that at 2.8 K coherent structures are obtained. In this case from their figure 1 we estimate a maximum of $\langle A_n \rangle$ at $n = n_0$ of $\simeq -0.07$ Å. For $T = 7.0$ K they observe that this coherent structure starts to break down, leading at 11.2 K to localized structures comparable to small polarons (this might also be interpreted as an Anderson localization originating from increasing disorder due to thermal fluctuations). For 7.0 K the maximum of $\langle A_n \rangle$ is found to be $\simeq -0.08$ Å and $\simeq -0.09$ Å for 11.2 K [23]. The latter value is already close to the infinite-temperature limit of $\simeq -0.095$ Å [23].

In figure 4 we show our results obtained with the $|D_1\rangle$ state and Davydov's model for temperature effects, but using correct equations of motion as given in the previous section. We followed the dynamics over a period of 6 ns, corresponding to 3 000 000 time steps. The calculation for one temperature had to be done in six runs, where only one of these six runs already requires 7.7 CPU hours computation time on a Cyber 995E computer from Control Data Corporation (500 000 time steps each run). Typically ($T = 11.2$ K) the error in total energy in such runs is $\simeq 3$ neV and the norm error is less than 0.05 ppm (parts per million). We see from figure 4(*a*) that at $T = 2.8$ K after roughly 1 ns a soliton nucleates from the random initial conditions and performs a random walk in the system. This corresponds qualitatively to the coherent structure found by Wang *et al* [23] at this temperature. At $T = 7.0$ K (figure 4(*b*)) also such a localized packet forms, but it is first of all smaller and after 2 ns it remains confined within a few lattice sites, again corresponding to the destruction of the coherent structure towards a localized state as reported in [23] for this temperature. Finally at 11.2 K (figure 4(*c*)) the packet remains in the middle of the chain and becomes smaller, again in qualitative agreement with [23]. Thus Davydov's model appears to be in qualitative agreement with quantum Monte Carlo results. However, it does not agree quantitatively as figure 5 shows, where we present the time average $\langle A_n \rangle$ of the lattice displacements through 3 000 000 time steps. Obviously the structure found has a decreasing width with increasing temperature, but the peak values are $\simeq -0.026$ Å (2.8 K), $\simeq -0.028$ Å (7.0 K) and $\simeq -0.029$ Å (11.2 K), in contrast to the much larger values found in [23] (-0.07, -0.08, -0.09 Å, respectively). Also the increase of this peak value with temperature is much less pronounced than in the quantum Monte Carlo case. Therefore we conclude that

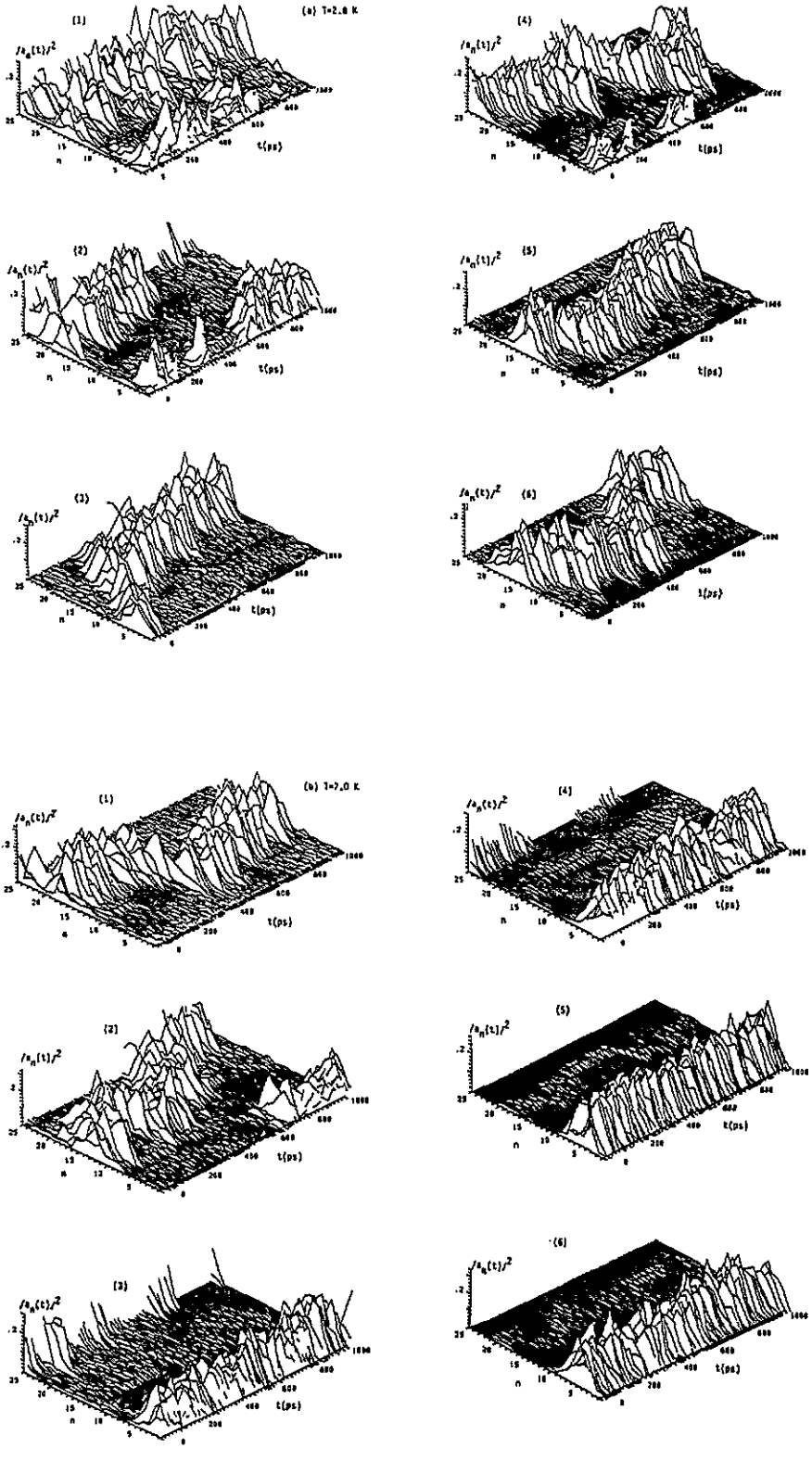
(a) T=2.8 K
(1)
(2)
(3)
(4)
(5)
(6)
t(ps)
n
(b) T=7.0 K
(1)
(2)
(3)
(4)
(5)
(6)
t(ps)
n

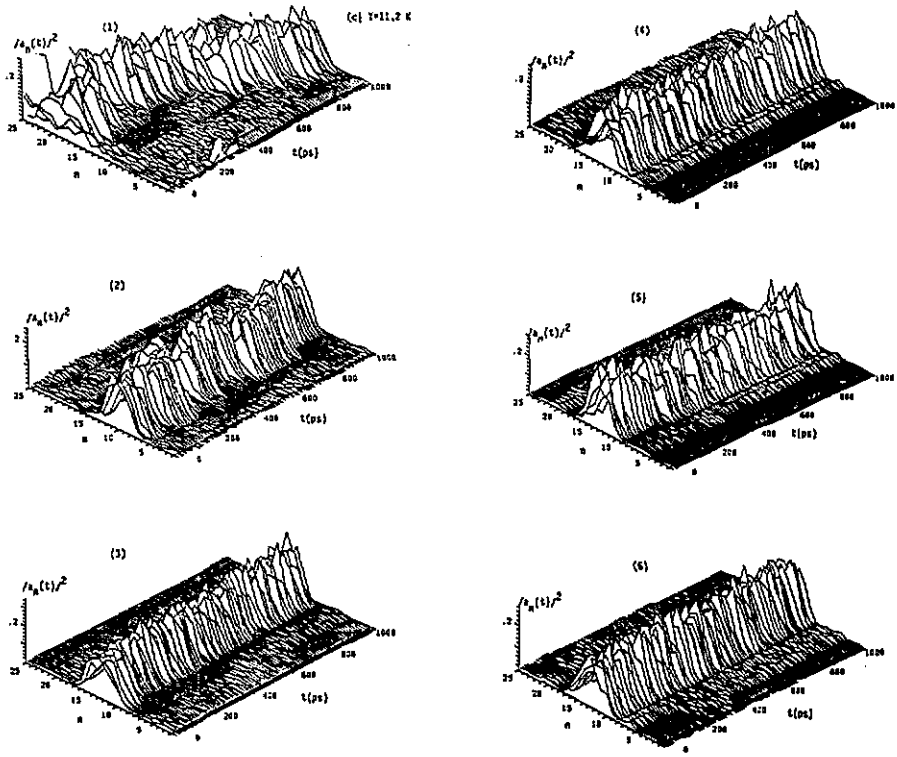

Figure 4. Time evolution of the excitation probability $|a_n(t)|^2$ from an initially randomly distributed amide-I quantum as function of site n and time t in cyclic chains of 25 units and with symmetric interaction, using the $|D_1\rangle$ *ansatz* state and Davydov's model for temperature effects. Each subfigure (1–6) shows every 5000th of 500 000 time steps ($\tau = 2$ fs). (*a*) $T = 2.8$ K; (*b*) $T = 7.0$ K; (*c*) $T = 11.2$ K.

Davydov's $|D_1\rangle$ model gives a qualitatively correct picture, but fails to reproduce exact results quantitatively.

Let us turn now to the partial dressing state of Brown and Ivic [17], which as mentioned above is a special case of the $|D_1\rangle$ *ansatz* with a fixed dependence of the coherent state amplitudes b_{nk} on the site n. Our simulations at 0 K for this state have shown that the results are qualitatively somewhat similar to $|D_1\rangle$ dynamics, but with dispersing solitary waves appearing at even higher values of X than in zero-temperature $|D_1\rangle$ theory [20]. In the case of this state already after 900 000 time steps of 2 fs convergence of the average $\langle A_n \rangle$ is obtained. The calculation time for one of the three temperatures is 8 CPU hours on the same computer as mentioned above. The energy is conserved (11.2 K) to better than 20 neV, and the norm to better than 11 ppm. Since in this case no solitons are nucleated, and in the $|a_n(t)|^2$ plots only random behaviour is seen, we show in figure 6 only the averages $\langle A_n \rangle$ for the three temperatures under consideration. We see immediately that in this case the values from [23] for the peak are underestimated by all three curves, even more strongly than in $|D_1\rangle$ theory. Thus even at 2.8 K, where in [23] coherent structures were found, the partial dressing *ansatz* shows a narrow and too small peak for all three temperatures. The peak does not change for increasing temperature and thus

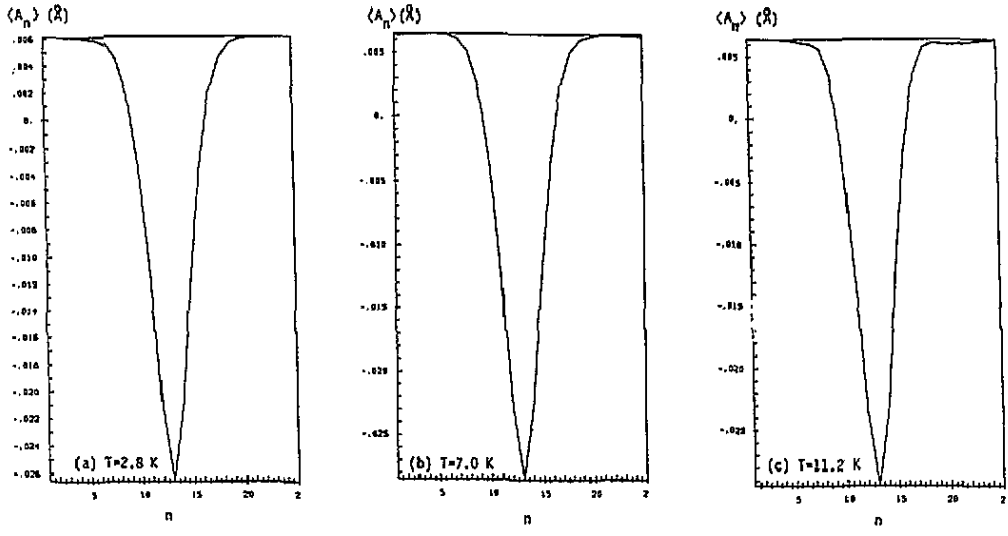

Figure 5. Time average $\langle A_n \rangle$ over 3 000 000 time steps (6 ns) of the lattice displacements A_n in the rotated coordinate system for the system of figure 4 at the same temperatures.

for this *ansatz* we do not even find qualitative agreement with quantum Monte Carlo results.

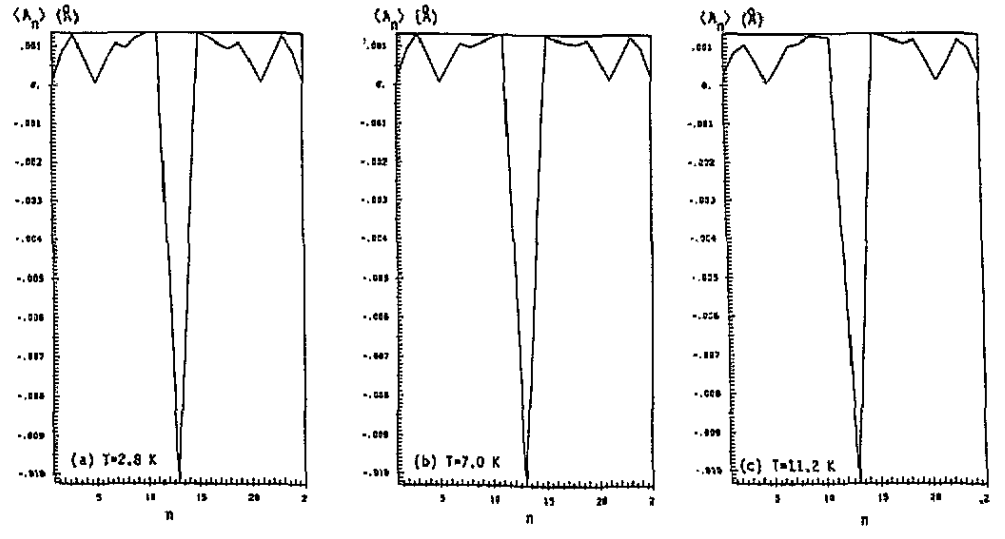

Figure 6. Same as figure 5 but using the partial dressing *ansatz* and averaging over only 900 000 time steps (1.8 ns).

In figure 7 we again present the average $\langle A_n \rangle$ over 12 000 000 time steps (12 ns) of 1 fs for the $|D_2\rangle$ *ansatz* with our temperature model. The norm was conserved to better than 0.09 ppm and the computation time was 21.7 CPU hours for one temperature. We see from the figure that in the $|D_2\rangle$ case the peak values of $\langle A_n \rangle$

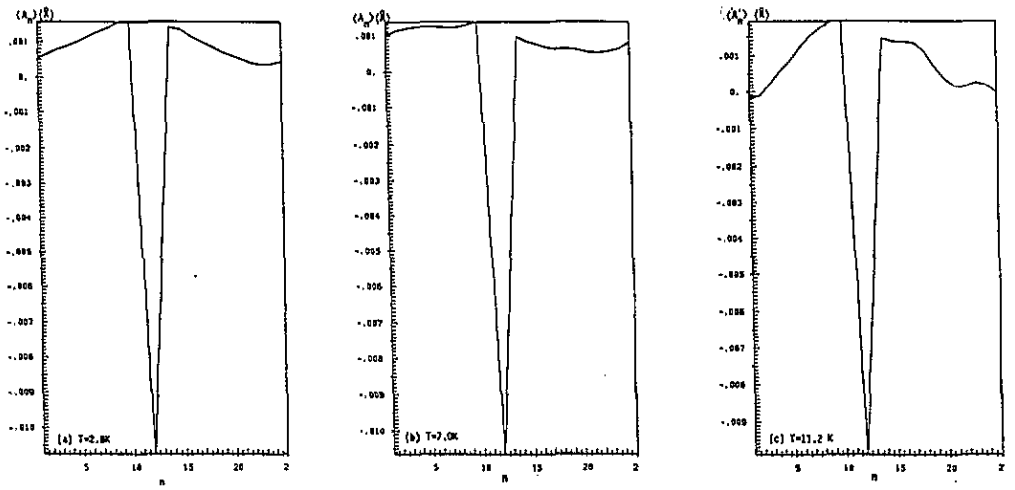

Figure 7. Same as figure 5 but using the $|D_2\rangle$ *ansatz*, our temperature model and averaging over 12 ns (12 000 000 time steps of 1 fs each).

are close to the corresponding $|D\rangle$ state values, but with the wrong tendency: they decrease somewhat with increasing temperature (2.8 K, −0.0107 Å; 7.0 K, −0.0106 Å; 11.2 K, −0.0098 Å). However, the decrease is not very pronounced. Since there are no solitary or small-polaron-like structures visible in the $|a_n|^2$ plots it seems that here the temperature effects are again strongly underestimated. Finally in figure 8 we show again the average quantity $\langle A_n \rangle$ for the $|D_2\rangle$ *ansatz* state but now using the Langevin equation model introduced by Lomdahl and Kerr. The time step size is again 1 fs and we averaged over 24 000 000 time steps (24 ns). The norm conservation (in the case of $T = 7.0$ K for example) was better than 1.5 ppb (parts per billion), the time average of the total kinetic energy divided by $0.5Nk_BT$ oscillated between 0.99 and 1.01 after equilibrium was reached, and the computation time was 24.0 CPU hours for one temperature. We see from the figure that the result is very close to that obtained with our model. The peak values are −0.0111 Å for 2.8 K, −0.0103 Å for 7.0 K and −0.0105 Å for 11.2 K. In all three cases $\langle A_n \rangle$ changed only in the range of roughly 0.1 mÅ between 16 000 000 and 24 000 000 time steps and thus was converged.

In conclusion it seems that, among the models studied, the $|D_1\rangle$ *ansatz* together with Davydov's treatment of temperature is the only one that gives an at least qualitatively correct picture, although it is quantitatively incorrect and furthermore there are doubts on the validity of Davydov's *ansatz* for the description of temperature. However, it seems that Davydov's *ansatz* can be viewed as a qualitatively valid approximation. But there is still a need for alternative models in order to overcome the conceptual difficulties with Davydov's *ansatz* and to arrive at quantitatively better approximations, although $|D_1\rangle$ theory is closest to QMC of all models studied.

5. Conclusions

With the classical $|D_2\rangle$ *ansatz* state we performed in previous work [11–13] dynamic simulations on one chain using different models for the incorporation of a finite

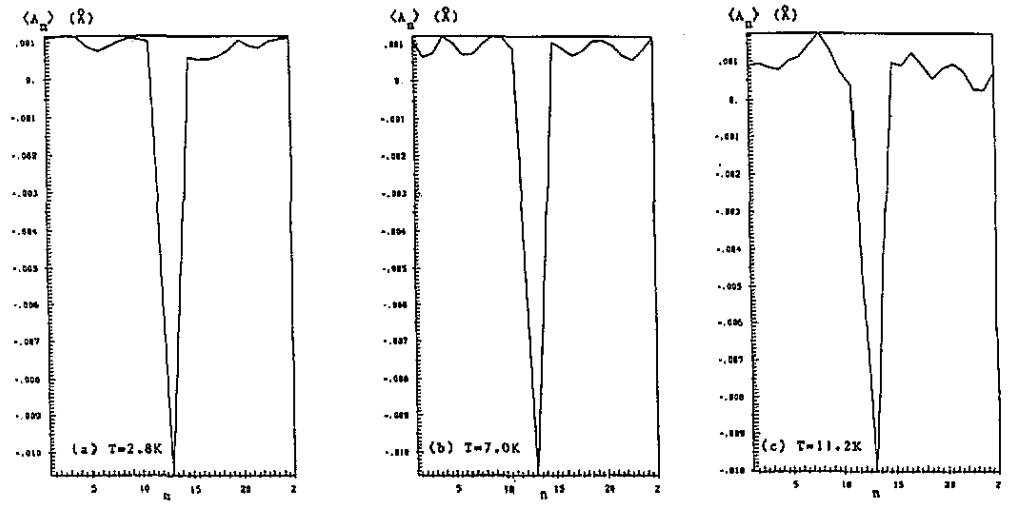

Figure 8. Same as figure 5 but using the $|D_2\rangle$ *ansatz*, the Langevin equation and an averaging over 24 ns (24 000 000 time steps of 1 fs each).

temperature into the Davydov soliton theory. We varied the parameters W (hydrogen-bond spring constant) and X (oscillator–lattice coupling constant). We found that at 300 K the spring constant of the hydrogen bonds should be larger than roughly 40 N m^{-1} to allow formation and propagation of Davydov solitons in the system. In calculations with the $|D_1\rangle$ *ansatz* state, which allows for quantum effects in the lattice and Davydov's method for incorporation of temperature, we arrived at roughly the same conclusion [21]. Since Davydov's method to account for temperature effects is believed by several workers to be inconsistent with statistical mechanics, we performed comparisons with exact quantum Monte Carlo results (QMC) [23]. Since these results are available only for one set of parameters and with the rather unrealistic symmetric interaction *ansatz*, we incorporated these features into our programs to be able to perform comparable calculations. Instead of the ensemble average in QMC we performed a time average over the lattice displacements in a rotated coordinate system. We found that the transition from coherent to localized structures between 2.8 and 11.2 K reported in [23] is reproduced by Davydov's method. However, quantitatively the averaged lattice displacements and their variation with temperature are underestimated. Thus the method serves as a qualitatively correct approximation to the dynamics at physiological temperature. The classical $|D_2\rangle$ *ansatz* underestimates temperature effects even more, while the partial dressing *ansatz* [17] leads neither to coherent structures below 7.0 K nor to localized ones above 7.0 K and also underestimates the averaged lattice displacements and their temperature variation.

If the spring constant of the hydrogen bonds in protein α-helices is larger than 30–40 N m^{-1} the Davydov soliton should be able to function at 300 K. Interestingly this conclusion is reached with both of Davydov's *ansatz* states and with different models for temperature effects. Since the usually quoted value of 13 N m^{-1} is derived from formamide crystals, where the hydrogen-bonded molecules vibrate freely, it should be too small for proteins. In proteins the hydrogen-bonded sites are embedded in the covalent backbone of the helix, which becomes distorted due to the vibration. Thus

we expect the spring constant of a protein normal mode corresponding to hydrogen-bond stretch to be much larger than that of crystalline formamide, and thus probably allowing for Davydov solitons to be formed in proteins. Further, following Scott (see e.g. [14]) the spring constant in one-chain simulations should be chosen larger anyway in order to resemble three-chain dynamics. The problem of interchain interactions is the subject of the following paper [26]. However, calculations or measurements on the spring constant in proteins are necessary to decide finally on the question of the existence of Davydov solitons.

Acknowledgments

The financial support of the 'Deutsche Forschungsgemeinschaft' (Project Ot 51/6-2) and the 'Fond der Chemischen Industrie' is gratefully acknowledged.

References

[1] Davydov A S and Kislukha N I 1973 *Phys. Status Solidi* b **59** 465
Davydov A S 1979 *Phys. Scr.* **20** 387
[2] Davydov A S 1980 *Zh. Eksp. Teor. Fiz.* **78** 789 (Engl. Transl. 1980 *Sov. Phys.-JETP* **51** 397)
[3] Careri G, Buontempo U, Galuzzi F, Scott A C, Gratton E and Shyamsunder E 1984 *Phys. Rev.* B **30** 4689
Eilbeck J C, Lomdahl P S and Scott A C 1984 *Phys. Rev.* B **30** 4703
[4] Fann W, Rothberg L, Roberson M, Benson S, Madey J, Etemad S and Austin R 1990 *Phys. Rev. Lett.* **64** 607
[5] Scott A C 1982 *Phys. Rev.* A **26** 57; 1984 *Phys. Scr.* **29** 279
MacNeil L and Scott A C 1984 *Phys. Scr.* **29** 284; 1985 *Phil. Trans. R. Soc.* A **315** 423
[6] Halding J and Lomdahl P S 1987 *Phys. Lett.* **124A** 37
[7] Lomdahl P S and Kerr W C 1985 *Phys. Rev. Lett.* **55** 1235; 1991 *Davydov's Soliton Revisited* ed P L Christiansen and A C Scott, NATO ASI, Ser. B, Physics, vol 243 (New York: Plenum)
[8] Lawrence A F, McDaniel J C, Chang D B, Pierce B M and Birge R R 1986 *Phys. Rev.* A **33** 1188
[9] Bolterauer H 1986 *Structure Coherence and Chaos* Proc. MIDIT 1986 Workshop (Manchester: Manchester University Press); 1991 *Davydov's Soliton Revisited* ed P L Christiansen and A C Scott, NATO ASI, Ser. B, Physics, vol 243 (New York: Plenum)
[10] Cottingham J P and Schweitzer J W 1989 *Phys. Rev. Lett.* **62** 1792
Schweitzer J W and Cottingham J P 1991 *Davydov's Soliton Revisited* ed P L Christiansen and A C Scott, NATO ASI, Ser. B, Physics, vol 243 (New York: Plenum)
[11] Motschmann H, Förner W and Ladik J 1989 *J. Phys.: Condens. Matter* **1** 5083
Förner W and Ladik J 1991 *Davydov's Soliton Revisited* ed P L Christiansen and A C Scott, NATO ASI, Ser. B, Physics, vol 243 (New York: Plenum) p 267
[12] Förner W 1991 *J. Phys.: Condens. Matter* **3** 3235, 4333
[13] Förner W 1992 *J. Comput. Chem.* **13** 275
[14] Scott A C 1993 *Phys. Rep.* at press
[15] Brown D W, Lindenberg K and West B J 1986 *Phys. Rev.* A **33** 4104, 4110; 1987 *Phys. Rev.* B **35** 6169; 1988 *Phys. Rev.* B **37** 2946
Brown D W 1988 *Phys. Rev.* A **37** 5010
[16] Cruzeiro L, Halding J, Christiansen P L, Skovgaard O and Scott A C 1988 *Phys. Rev.* A **37** 880
[17] Brown D W and Ivic Z 1989 *Phys. Rev.* B **40** 9876
[18] Förner W 1991 *Phys. Rev.* A **44** 2694; 1992 *J. Mol. Struct.* at press
[19] Mechtly B and Shaw P B 1988 *Phys. Rev.* B **38** 3075
[20] Skrinjar M J, Kapor D V and Stojanovic S D 1988 *Phys. Rev.* A **38** 6402
[21] Förner W 1992 *J. Phys.: Condens. Matter* **4** 1915
[22] Förner W 1993 *Nanobiology* **1** at press
[23] Wang X, Brown D W and Lindenberg K 1989 *Phys. Rev. Lett.* **62** 1796

[24] Kerr W C and Lomdahl P S 1987 *Phys. Rev.* B **35** 3629
[25] Kerr W C and Lomdahl P S 1991 *Davydov's Soliton Revisited* ed P L Christiansen and A C Scott, NATO ASI, Ser. B, Physics, vol 243 (New York: Plenum)
[26] Förner W 1993 *J. Phys.: Condens. Matter* **5** 823